Supporting Information

Interface Engineering: Few-Layered MoS_2 Coupled on NiCo-Sulfide Nanosheet Heterostructure as Bifunctional Electrocatalyst for Overall Water Splitting

Congli Qin, Aixin Fan, Xin Zhang,* Shiqing Wang, Xiaolin Yuan, and Xiaoping Dai

Experimental Section

Synthesis of NiCo-MOF nanosheet: $Ni(NO_3)_2 \cdot 6H_2O$ (0.5 mmol) and $Co(NO_3)_2 \cdot 6H_2O$ (0.5 mmol) were mixed with 20 mL of methanol solution to form solution A. 2-methyl imidazole (4 mmol) was dissolved in 20 mL of methanol solution to form solution B. Then solution B was added quickly into solution A. The mixture was then transferred into a Teflon-lined autoclave and reacted at 140 °C for 12 h. The resultant precipitate was rinsed and dried under vacuum for further use.

Synthesis of MoS_2/NiCoS nanosheet: NiCo-MOF nanosheet (30 mg) and ammonium thiomolybdate (10 mg) were put into 15 mL of N, N-dimethylformamide (DMF) with the assistance of ultrasonication for 30 min. Then the mixture was transferred into a 30 mL autoclave and reacted at 200 °C for 24 h. The resultant precipitate was washed and dried under vacuum overnight. Bare MoS_2 was prepared by the same method as MoS_2/NiCoS nanosheet, except for the addition of NiCo-MOF nanosheet.

Electrode preparation and electrochemical tests: CHI 760E electrochemistry workstation was used for electrochemical experiments with a conventional three-electrode system at room temperature. A mercuric oxide electrode (SME) was used as the reference electrode, a carbon rod was employed for the counter electrode and a glassy carbon (GC) electrode (3 mm in diameter) acted as the working electrode. All potentials obtained from OER and HER were converted to the reversible hydrogen electrode (RHE) according to the following equations: $E_{RHE} = E_{SME} + E^{\theta}_{SME} + 0.059$ pH. The preparation of working electrode was used by the following method: 2 mg of catalyst was mixed into a mixture of 200 μL of ethanol and 800 μL of deionized water with 10 μL of Nafion (5 wt%) with sonication for 40 min. Subsequently, 5 μL of suspension was dropped onto the surface of GC and dried at room temperature.

The loading amount of the catalyst is ~0.14 mg cm^{-2}. Linear sweep voltammetry (LSV) was measured at a scan rate of 5 mV s^{-1}. Electrochemical impedance spectra (EIS) were recorded in the frequency range from 0.01 to 10^5 Hz. All polarization curves were corrected with 95% iR-compensation.[1,2] For the over water splitting, Ni foam (NF, 1 × 1 cm) was utilized as the working electrode with an approximate catalyst loading of ~3 mg·cm^{-2}. For the over water splitting, Ni foam (NF, 1 × 1 cm) was utilized as the working electrode. The Ni foam was cleaned by sonication sequentially in acetone, 1.0 M HCl solution and water for 30 min each. 3 mg of catalyst was suspended in a mixture of 200 μL of ethanol and 800 μL of deionized water with 10 μL of Nafion (5 wt%) solution to form a homogeneous catalyst ink by sonication for 30 min. Then, the uniform suspension was dropped on Ni foam and left to dry in air (this yielded an approximate metal loading of ~3 mg on Ni foam).

The values of ECSA was calculated based on previous reported:[3–5]

$$ESCA = \frac{C_{dl}}{C_s}$$

Where, the C_s is the specific capacitance in the range of 0.020−0.090 mF cm^{-2}. The capacitance of 0.040 mF cm^{-2} was used to calculate the ECSA based on typical reported values.

The TOF was calculated by the following equation:

$$TOF = \frac{j \times A}{m \times F \times n}$$

where, J (mA cm^{-2}) is the measured current density at given overpotential; A is the surface area of GC electrode (0.07065 cm^2); m is the number of electrons (OER m=4 and HER m=2); F is faraday constant (96485.3 C mol^{-1}) and n is the total mole of the metal atoms on the electrode (assuming that every metal atom is involved in the catalysis).

Characterization: Transmission electron microscopy (TEM) analysis was determined by JEM-2100 at 200 kV. High-resolution transmission electron microscope HRTEM and high-angle annular dark-field scanning TEM (HAADF-STEM) were observed on a Tecnai G^2 F20 S-Twin at 200 kV. The scanning electron microscope (SEM) images were determined by an ULTRA 55 SEM at 20 kV. Power X-ray

diffraction (XRD) was performed on a Brüker D8 Advance diffractometer at 40 kV and 40 mA for Cu Kα (λ= 0.15406). The Raman spectra were determined on a HORIBA Jobin Yvon HR800. X-ray photoelectron spectroscopy (XPS) was measured by an X-ray photoelectron spectrometer (PHI 5000 Versaprobe) with monochromatic Al Kα radiation (1486.6 eV). The amount of Ni, Co and S was measured by inductively coupled plasma optical emission spectrometry (ICP-OES).

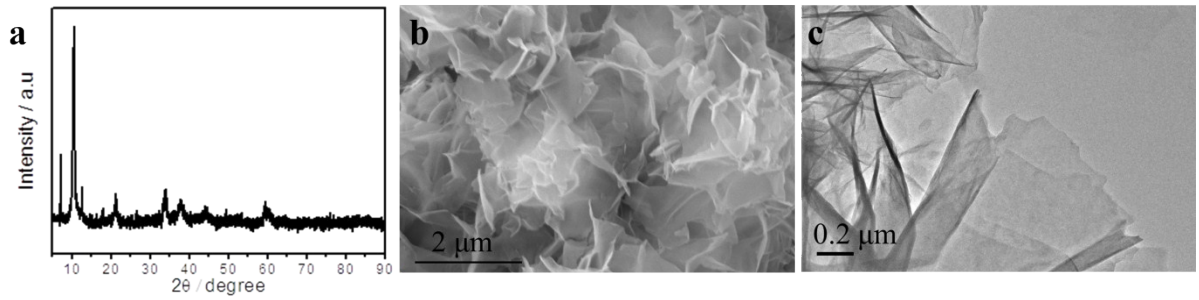

Figure S1 (a) XRD pattern, (b) SEM and (c) TEM image of NiCo-MOF nanosheet.

58 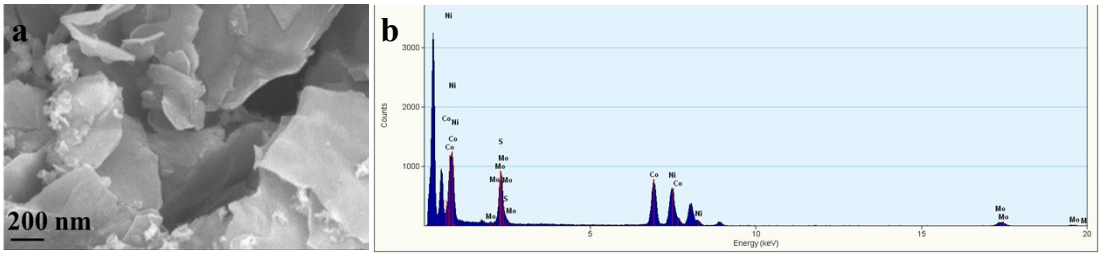

59 **Figure S2** (a) SEM image and (b) EDX spectrum of MoS_2/NiCoS heterostructure.

60

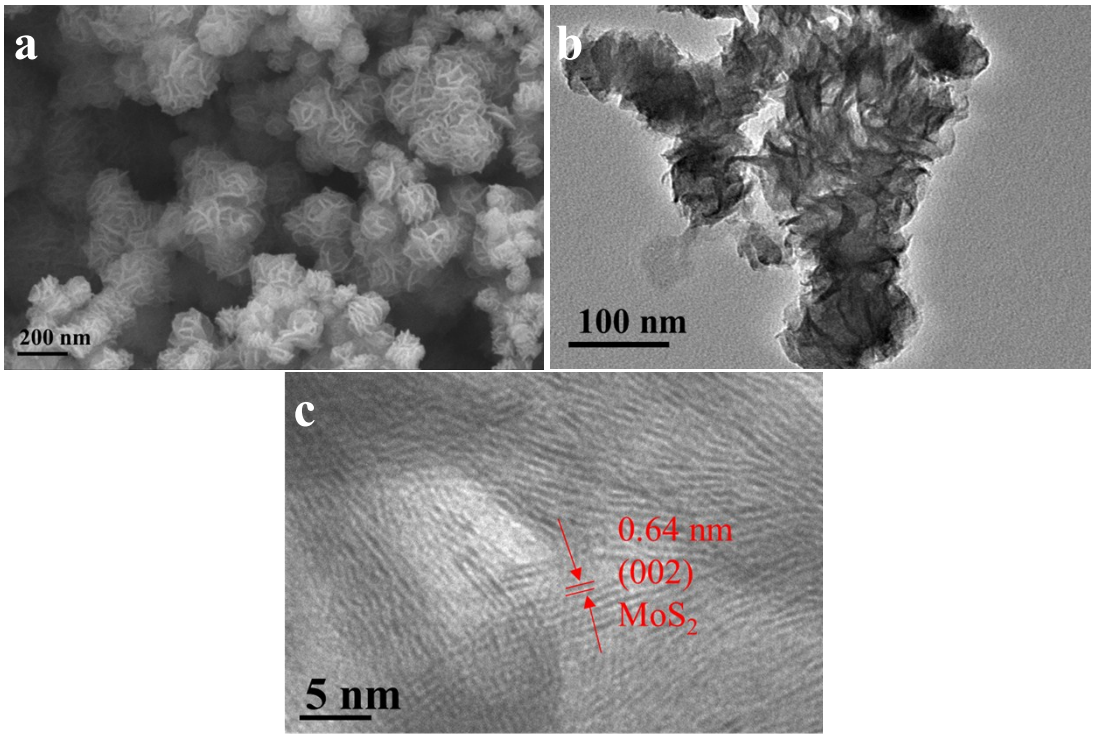

Figure S3 (a) SEM and (b, c) TEM images of bare MoS_2.

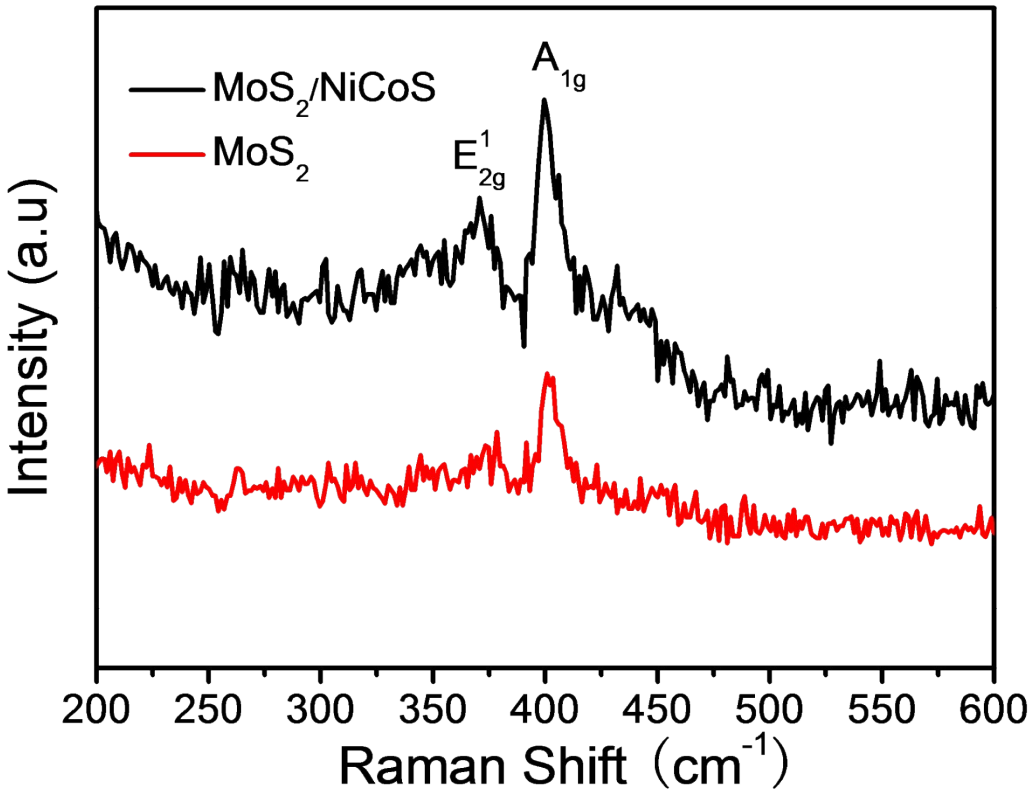

64

65 **Figure S4** Raman spectra of MoS_2/NiCoS heterostructure and bare MoS_2.

66

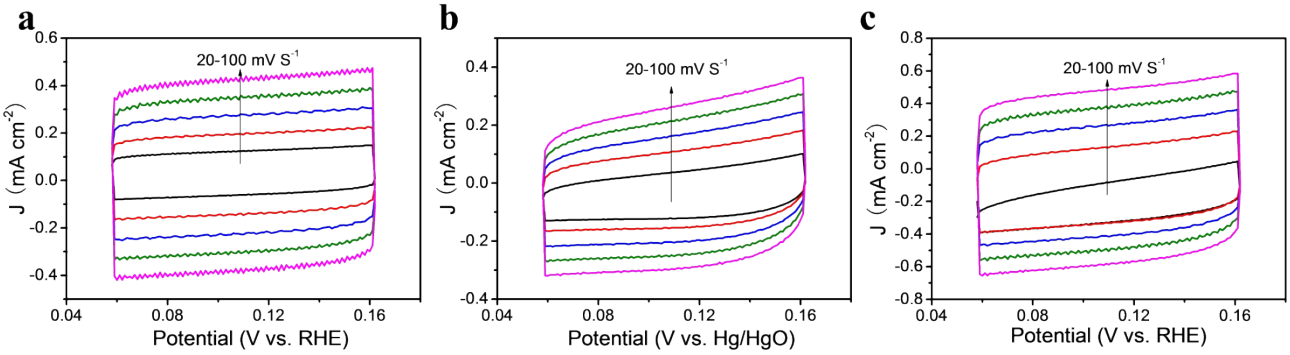

Figure S5 Cyclic voltammetry in non-faradaic potential at different scan rates (20, 40, 60, 80, and 100 mV s^{-1}) for (a) MoS_2, (b) NiCoS and (c) MoS_2/NiCoS.

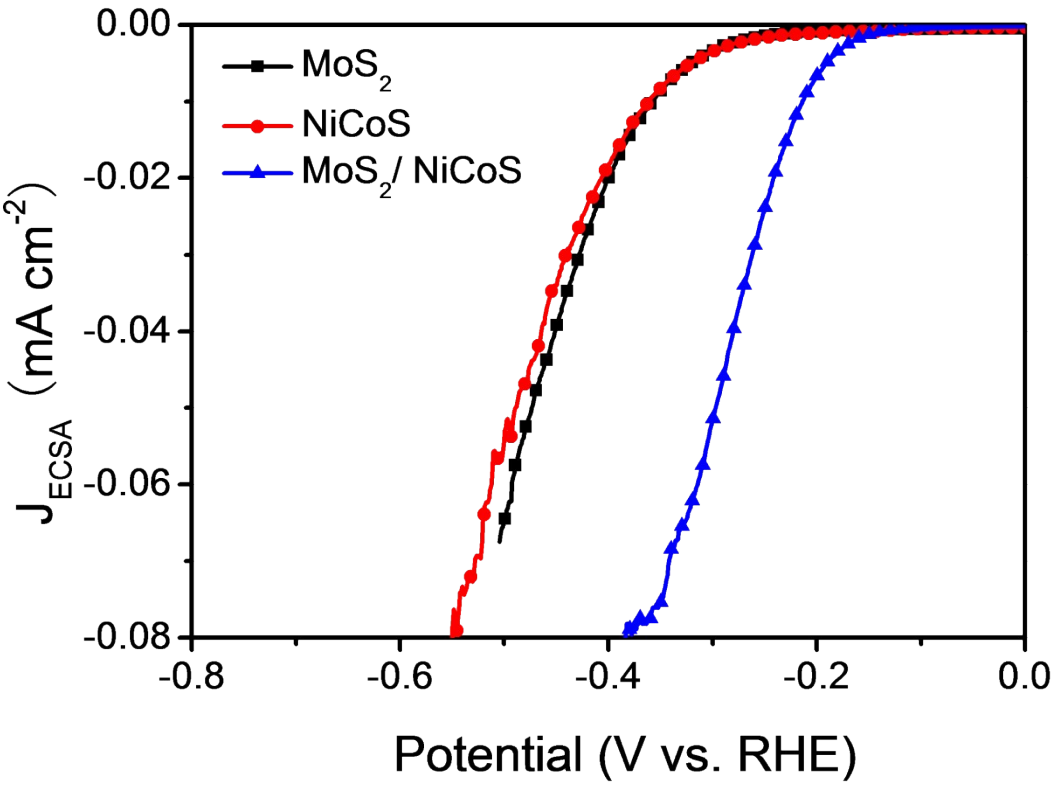

71

72 **Figure S6** LSV curves of the as-synthesized catalysts normalized by ECSA.

73

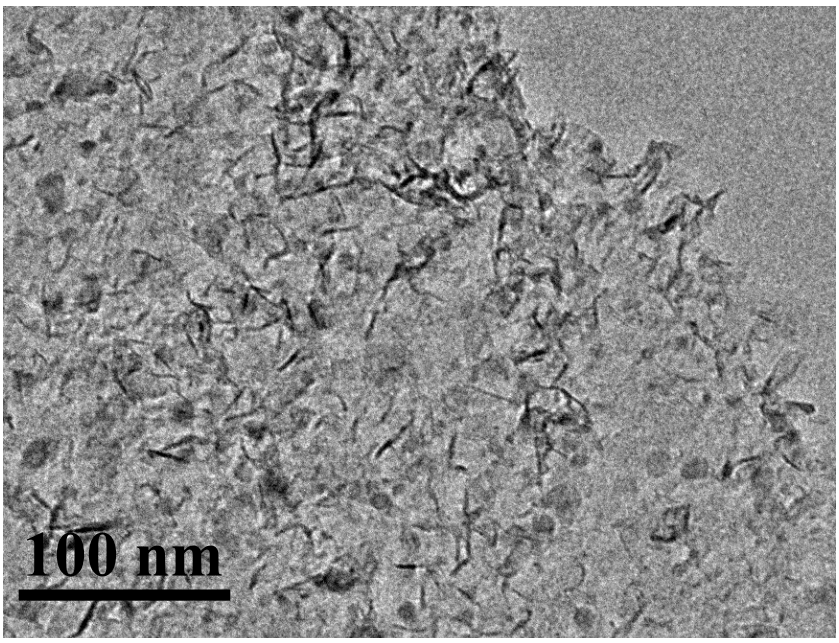

Figure S7 TEM image of the MoS_2/NiCoS after HER durability test. The structure of MoS_2/NiCoS is stable after the HER durability test.

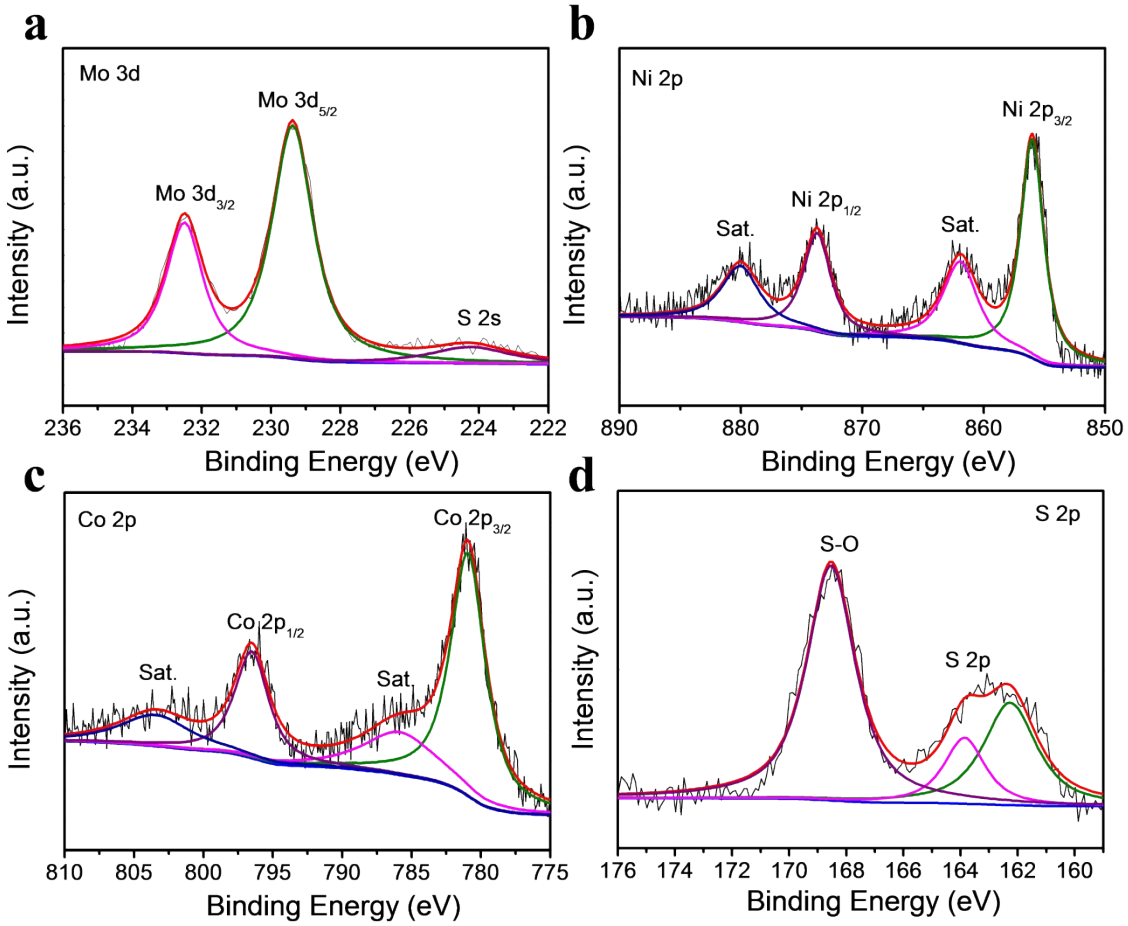

77

78 **Figure S8** High-resolution XPS spectra (a) Mo 3d, (b) Ni 2p, (c) Co 2p, and (d) S 2p of MoS_2/NiCoS

79 nanosheet after HER test.

80

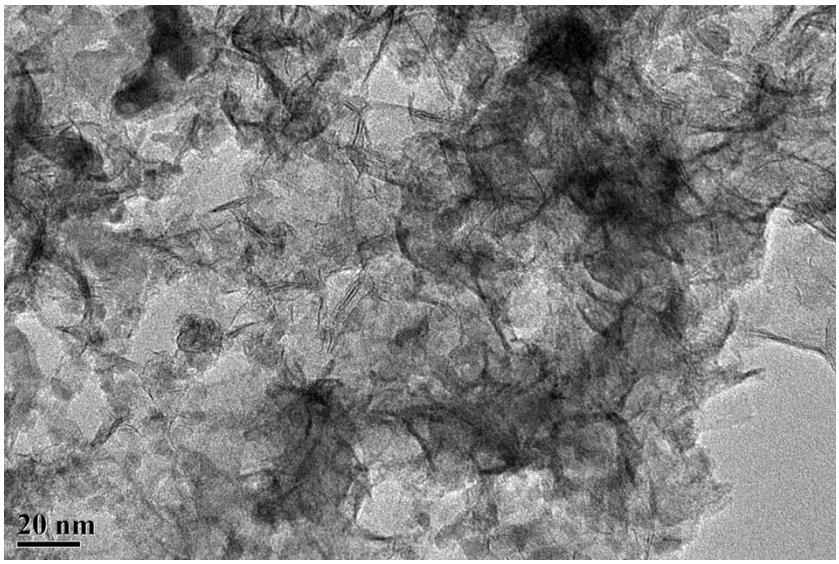

Figure S9 TEM image of the MoS_2/NiCoS after OER durability test. The structure of MoS_2/NiCoS is stable after the OER durability test.

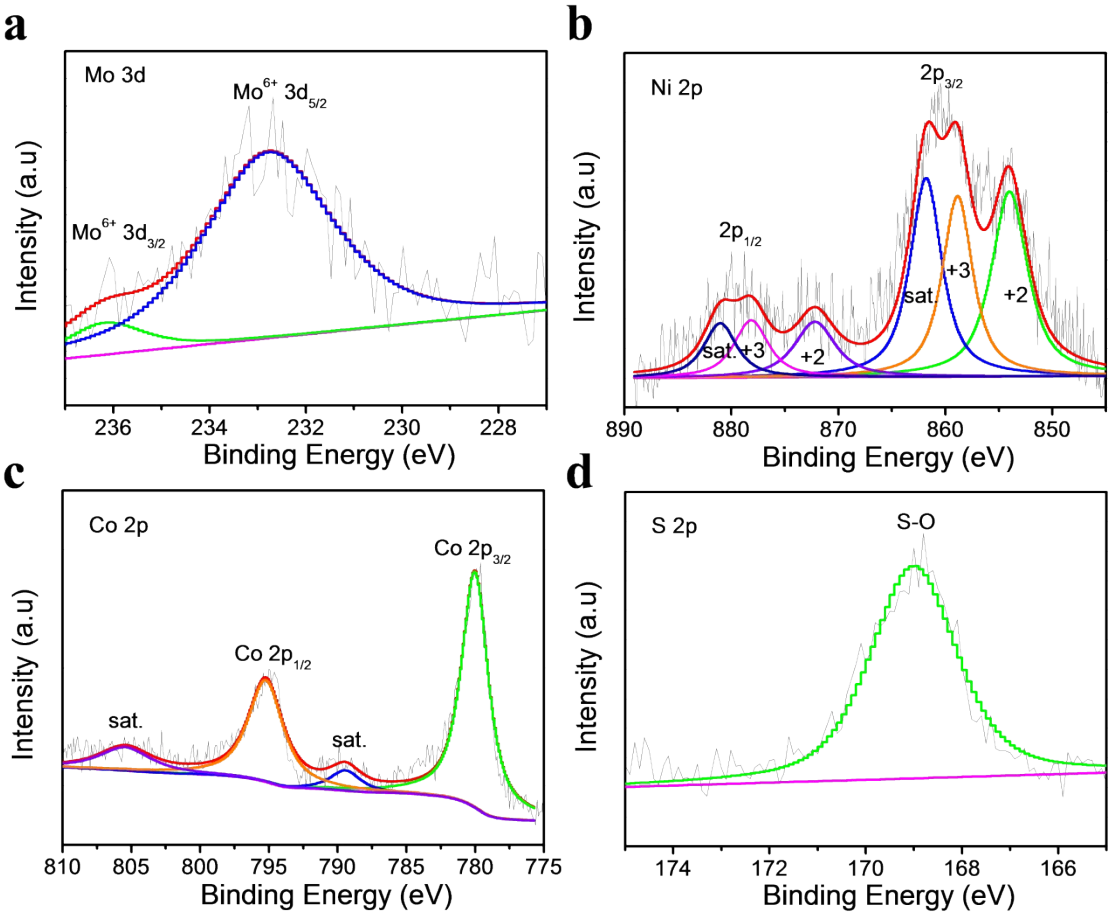

84

85 **Figure S10** High-resolution XPS spectra (a) Mo 3d, (b) Ni 2p, (c) Co 2p, and (d) S 2p of MoS_2/NiCoS

86 nanosheet after OER test.

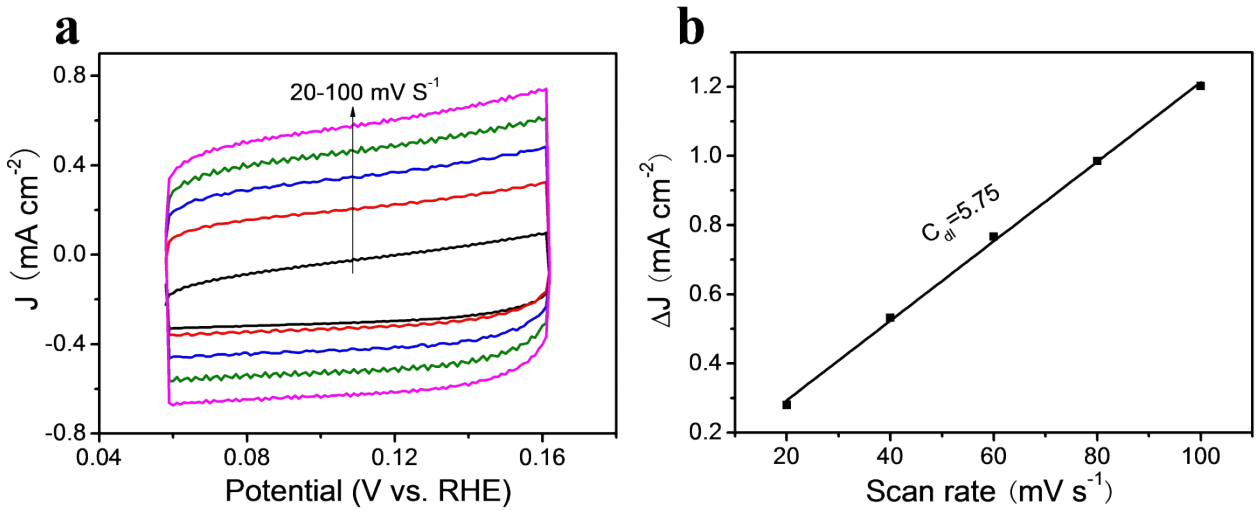

Figure S11 (a) Cyclic voltammetry in non-faradaic potential at different scan rates (20, 40, 60, 80, and 100 mV s^{-1}) and (b) Linear fitting of the capacitive currents *vs* CVs scan rate for MoS_2-NiCoS.

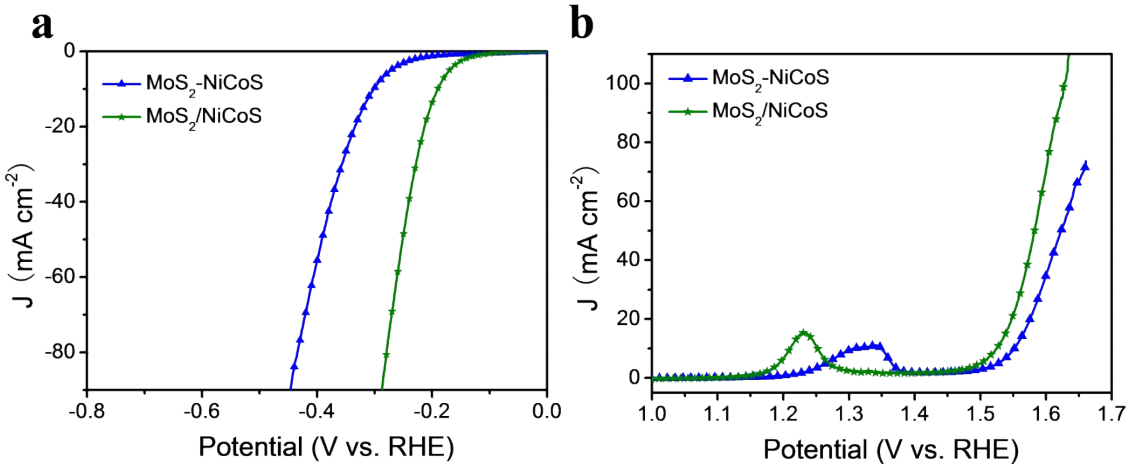

91

92 **Figure S12** LSV of MoS_2-NiCoS and MoS_2/NiCoS for (a) HER and (b) OER.

93

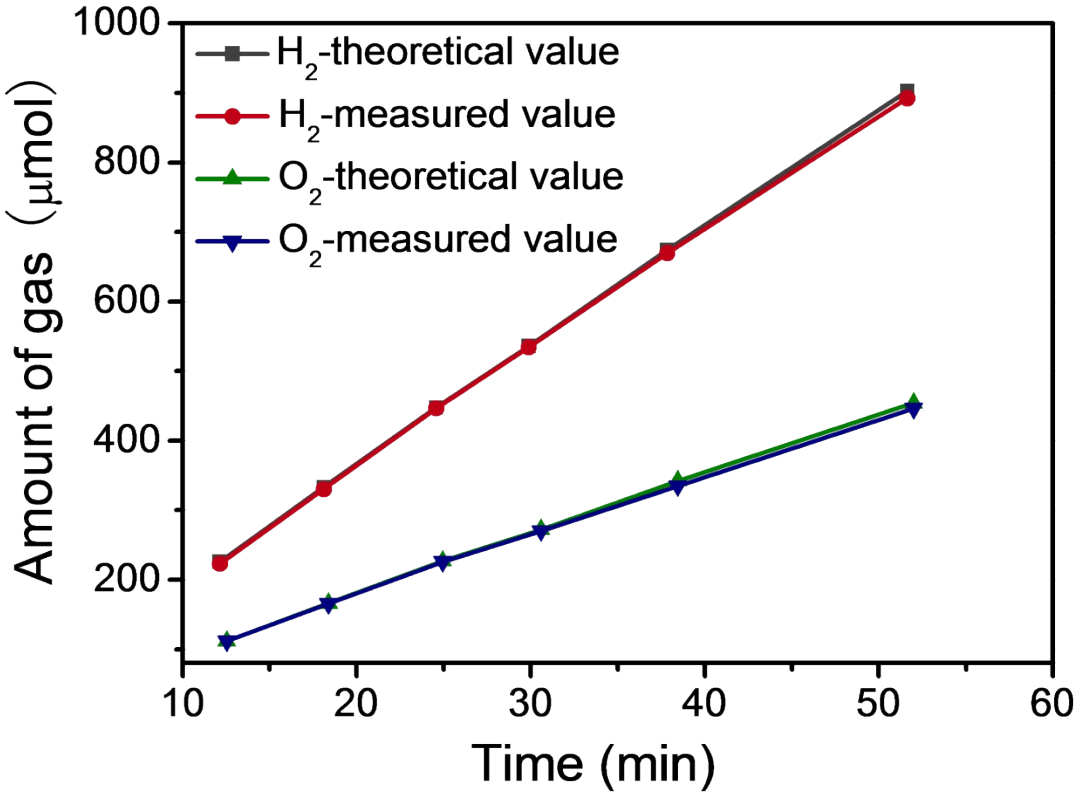

Figure S13 The experimental and theoretical H_2 and O_2 amounts in different time for overall water splitting of MoS_2/NiCoS heterostructure nanosheets.

Table S1 Comparison of HER performance for MoS_2/NiCoS with other non-noble metal electrocatalysts tested in alkaline solution.

Catalysts	Loading mg/cm^{-2}	Substrate	Electrolyte	η (mV) 10 mA/cm^{-2}	Tafel slope mV/decade	Reference
MoS_2/NiCoS	0.14	GC	1.0 M KOH	189	75	This work
MoS_2/NiS	0.234	GC	1.0 M KOH	244	97	6
Mo-W-S-2@Ni_3S_2	-	Ni foil	1.0 M KOH	98	92	7
CoSx@MoS_2	0.5	Ni foil	1.0 M KOH	146	56.51	8
MoS_2/Ni_3S_2	9.7	Ni foil	1.0 M KOH	110	83	9
$CoMoS_{3.13}$-12h	0.5	Ni foil	1.0 M KOH	190	-	10
MoS_2@CoO	2.0	carbon cloth	1.0 M KOH	173	83	11
Co_4Mo_2@NC	0.357	GC	1.0 M KOH	218	73.5	12
NiS_2/MoS_2	0.2	GC	1.0 M KOH	204	65	13
Co_3S_4-L	0.42	GC	1.0 M KOH	270	124.5	14

101 **Table S2** Composition of MoS_2, NiCoS, and MoS_2/NiCoS determined by ICP-OES.

	MoS_2	NiCoS	MoS_2/NiCoS
Mo (wt%)	41.2	-	12.1
Ni (wt%)	-	23.8	29.5
Co (wt%)	-	24.5	28.1

103 **Table S3** OER data summarized from as-synthesized samples.

Catalyst	**η at j = 10 mA cm^{-2} (mV)**	**Tafel slope (mV dec^{-1})**	**mass activity at η = 350 mV (A g^{-1})**	**TOF at η = 350 mV (s^{-1})**
MoS_2	390	118	27.1	0.016
NiCoS	330	83	121.4	0.038
MoS_2/NiCoS	290	77	340	0.080

104

Table S4 Comparison of OER performance for MoS_2/NiCoS with other non-noble metal electrocatalysts tested in alkaline solution.

Catalysts	Loading mg/cm^{-2}	Substrate	Electrolyte	η (mV) 10 mA/cm^{-2}	Tafel slope mV/decade	Reference
MoS_2/NiCoS	0.14	GC	1.0 M KOH	290	77	This work
MoS_2/NiS	0.234	GC	1.0 M KOH	350	108	6
Mo-W-S-2@Ni_3S_2	-	Ni foil	1.0 M KOH	285	98	7
CoSx@MoS_2	0.5	Ni foil	1.0 M KOH	276	26.08	8
MoS_2/Ni_3S_2	9.7	Ni foil	1.0 M KOH	218	88	9
$CoMoS_{3.13}$-12h	0.5	Ni foil	1.0 M KOH	280	-	10
MoS_2@CoO	2.0	carbon cloth	1.0 M KOH	325	129.9	11
Co_4Mo_2@NC	0.357	GC	1.0 M KOH	330	48.7	12
Co_9S_8-NSC@Mo_2C	0.425	GC	1.0 M KOH	293	59.7	15
$CuCo_2S_4$	0.7	GC	1.0 M KOH	310	86	16

Table S5 Compositions of holey MoS_2/NiCoS nanosheets before and after OER test.

	Before OER	After OER
Mo (wt%)	12	4
Ni (wt%)	26	29
Co (wt%)	28	34
S (wt%)	17	4
O (wt%)	14	27

Table S6 Comparison of water splitting performance for MoS_2/NiCoS with other non-noble metal electrocatalysts tested in alkaline solution.

Catalysts	Electrolyte	Substrate	Current density (mA/cm^2)	Voltage (V)	Reference
MoS_2/NiCoS	1.0 M KOH	NF	20	1.54	This work
MoS_2/NiS	1.0 M KOH	NF	10	1.64	6
Mo-W-S-2@Ni_3S_2	1.0 M KOH	NF	10	1.62	7
CoSx@MoS_2	1.0 M KOH	NF	10	1.668	8
Mo-W-S-2@Ni_3S_2	1.0 M KOH	NF	10	1.56	9
$CoMoS_{3.13}$-12h	1.0 M KOH	NF	10	1.574	10
Co_4Mo_2@NC	1.0 M KOH	Ti plate	10	1.74	12
Co_9S_8@MoS_2	1.0 M KOH	NF	10	1.67	17
$NiCo_2S_4$/NF	1.0 M KOH	NF	10	1.63	18
Co–Mo_2C@NCNT	1.0 M KOH	NF	10	1.628	19

Reference

1 Q. Wang, L. Shang, R. Shi, X. Zhang, Y. Zhao, G. I. N. Waterhouse, L. Wu, C. Tung and T. Zhang, *Adv. Energy Mater.*, 2017, **7**, 1700467.

2 Z. Fang, L. Peng, H. Lv, Y. Zhu, C. Yan, S. Wang, P. Kalyani, X. Wu and G. Yu, *ACS Nano*, 2017, **11**, 9550–9557.

3 C. Luan, G. Liu, Y. Liu, L. Yu, Y. Wang, Y. Xiao, H. Qiao, X. Dai and X. Zhang, *ACS Nano*, 2018, **12**, 3875–3885.

4 C. C. L. McCrory, S. Jung, J. C. Peters and T. F. Jaramillo, *J. Am. Chem. Soc.*, 2013, **135**, 16977–16987.

5 C. Wei, C. Liu, L. Gao, Y. Sun, Q. Liu, X. Zhang and J. Guo, *J. Alloys Compd.*

6 Q. Qin, L. Chen, T. Wei and X. Liu, *Small*, 2019, **15**, 1803639.

7 M. Zheng, J. Du, B. Hou and C.-L. Xu, *ACS Appl. Mater. Interfaces*, 2017, **9**, 26066–26076.

8 S. Shit, S. Chhetri, S. Bolar, N. C. Murmu, W. Jang, H. Koo and T. Kuila, *ChemElectroChem*, 2019, **6**, 430–438.

9 J. Zhang, T. Wang, D. Pohl, B. Rellinghaus, R. Dong, S. Liu, X. Zhuang and X. Feng, *Angew. Chemie Int. Ed.*, 2016, **55**, 6702–6707.

10 S. Shit, W. Jang, S. Bolar, N. C. Murmu, H. Koo and T. Kuila, *ACS Appl. Mater. Interfaces*.

11 P. Cheng, C. Yuan, Q. Zhou, X. Hu, J. Li, X. Lin, X. Wang, M. Jin, L. Shui and X. Gao, *J. Phys. Chem. C*, 2019, **123**, 5833–5839.

12 J. Jiang, Q. Liu, C. Zeng and L. Ai, *J. Mater. Chem. A*, 2017, **5**, 16929–16935.

13 P. Kuang, T. Tong, K. Fan and J. Yu, *Acs Catal.*, 2017, **7**, 6179–6187.

14 M. Zhu, Z. Zhang, H. Zhang, H. Zhang, X. Zhang, L. Zhang and S. Wang, *J. Colloid Interface Sci.*, 2018, **509**, 522–528.

15 X. Luo, Q. Zhou, S. Du, J. Li, J. Zhong, X. Deng and Y. Liu, *ACS Appl. Mater. Interfaces*, 2018, **10**, 22291–22302.

16 M. Chauhan, K. P. Reddy, C. S. Gopinath and S. Deka, *ACS Catal.*, 2017, **7**, 5871–5879.

17 J. Bai, T. Meng, D. Guo, S. Wang, B. Mao and M. Cao, *ACS Appl. Mater. Interfaces*, 2018, **10**, 1678–1689.

18 A. Sivanantham, P. Ganesan and S. Shanmugam, *Adv. Funct. Mater.*, 2016, **26**, 4661–4672.

19 L. Ai, J. Su, M. Wang and J. Jiang, *ACS Sustain. Chem. Eng.*, 2018, **6**, 9912–9920.